

RGB lasers for laser projection displays

Günter Hollemann^a, Bernd Braun^a, Friedhelm Dorsch^b,
Petra Hennig^b, Peter Heist^a, Ulf Krause^a, Uwe Kutschki^a, Herrmann Voelckel^b

^aJENOPTIK Laser, Optik, Systeme GmbH, Göschwitzer Str. 25, D07745 Jena (Germany)

^bJENOPTIK Laserdiode GmbH, Prüssingstr. 41, D-07745 Jena (Germany)

ABSTRACT

JENOPTIK Laser, Optik, Systeme GmbH has developed the first industrial all-solid-state Red-Green-Blue laser system for large image projection systems. Compact in design (0.75 m³, 180 kg, 3 kW power consumption), the system consists of a modelocked oscillator amplifier subsystem with 7 ps pulse duration and 85 MHz pulse repetition frequency, an optical parametric oscillator (OPO), and several non-linear stages to generate radiation at 628 nm, 532 nm and 446 nm with an average output power above 18 W. Each of the three colors is modulated with the video signal in a contrast ratio of 1000:1 and coupled into a common low order multi mode fiber. The system architecture relies on efficiently manufacturable components. With the help of FEM analysis, new engineering design principles and subsequent climatic and mechanical tests, a length stability below 50 μm and an angle stability below 10 μrad have been achieved. The design includes efficient laser diodes with integrated thermo-electric cooler and a life time above 10000 hours. The stability of the output power is better than $\pm 2\%$ in a temperature range from 5 °C to 40 °C. The system operates reliably for more than 10,000 hours under field conditions. The design is based (among others) on work by Laser-Display-Technologie KG and the University of Kaiserslautern.

Keywords: Red-Green-Blue Laser, Modelocked Laser, Optical Parametric Oscillator (OPO), Laser Projection Display

1. INTRODUCTION

A practically unrestricted depth of focus, excellent color saturation, high contrast ratio and high resolution in combination with various video standards are the major advantages of laser projection systems compared to conventional lamp projectors. Each individual pixel is created by collinear superposition of three collimated laser beams in the image. By consequence, the image stays also properly focused if the distance to the projector is varying or inclined or if curved surfaces are used as a projection screen. The laser wavelengths used cover more than 90 % of all colors which are perceptible by the human eye (**Fig. 1**).

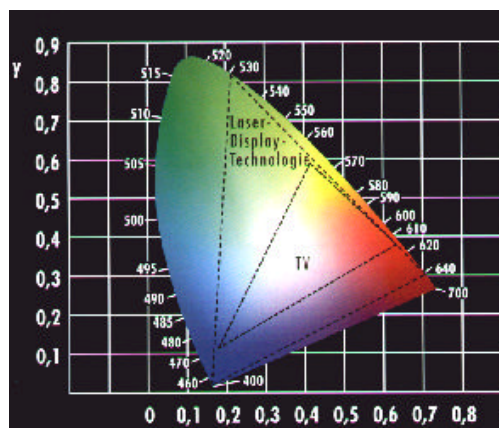


Fig. 1 Comparison of the color triangle of laser projection systems and traditional TV.

This is a significant improvement compared to conventional cathode emitter tubes (cathode-ray TV tube). The laser radiation is characterized by its high spectral purity (small spectral linewidth) and its precise wavelength given by the atomic laser transition. For this reason, the color triangle remains stable without any readjustment, once generated, and white balancing can automatically be achieved by adjustment of the laser output powers for red, green and blue. Rapid advancement in the field of high power laser diodes in the 90ties has turned the idea of laser television into reality. Compared with laser projection systems for large image projection based on Argon-ion lasers which required an electrical power of more than 100 kW, solid state lasers provide higher light output with a power consumption below 3 kW.

The dream of a laser television for home cinema will come true when RGB semiconductor lasers can be applied directly. The laser power required for home cinemas is in the order of several hundred mW up to one W per color. For a projection area of some tens of square meters, as required for projection in e-cinemas, planetarium or flight simulators etc., a laser power in the range of 5 to 20 W per color is required.

Therefore the demand for a highly effective and power-scaleable laser architecture provided the starting point for efforts to design an all-solid-state RGB laser system. This challenge is being met under a development scheme for an RGB laser with optical parametric oscillator pursued in recent years by R. Wallenstein and coworkers at the University of Kaiserslautern¹ and brought to sophistication by Laser-Display-Technologie KG (LDT) in Gera, Germany.

This paper reports on some results of developing a similar system to the industry-standard level. Various system components from color generation to modulation of the laser beams are described. The essential specifications of the laser light source are listed in **Table 1**.

Parameter	Specification
Power	
446 nm	> 4.8 W
532 nm	> 6.5 W
628 nm	> 7.0 W
Pulse duration	< 7 ps
Pulse repetition frequency	> 80 MHz
Beam quality M ²	< 1.5
Polarization	> 100:1 (linear)
Contrast ratio	> 1,000 : 1
Power stability	< +/- 2 % over 8 h
Amplitude noise	< 2 % RMS
Modulation frequency	32 MHz
Expected lifetime	10000 h/5 years
Electrical requirements	110 V/230 V, < 3 kW, 50 Hz/60 Hz
Mechanical requirements	Transportation on cars, ships and airplane
Dimensions, weight	1140*1150*600 mm ³ , 180 kg
Environmental requirements	
storage temperature range	- 25 °C ... + 70 °C
operating temperature range	+ 5 °C ... + 40 °C
humidity	65 +/- 15 % at 25 °C
Standards	EN 60825-1, EN 60950, EN 50081(82)-1 class B, ISO 9000, CE

Table 1 Specifications of the RGB laser system

A modular structure based on individual, detachable and exchangeable subsystems is a prerequisite for serial manufacturing, testing and servicing of the complete laser system. In line with the modular structure, the modules and various subsystems are described in more detail. Besides the physical principles and main characteristics emphasis is on stability of the modules.

The RGB laser system consists of a fiber coupled diode laser pump module, a power supply, a diode current supply, a diode plug-in unit with a control subsystem, a cooling unit and a laser head. The complete RGB laser system is shown in Fig. 2.



Fig. 2 RGB Laser System with dimensions of 1140*1150*600 mm³

The laser head consists of six stages, a diode-pumped oscillator, a diode-pumped amplifier, an optical parametric oscillator, a non-linear frequency stage, a delay unit and a modulation unit with acoustooptic modulation, white color balancing and fiber coupling (Fig. 3). Modelocked pulses with a full-width-at-half-maximum (FWHM) of 7 ps and a wavelength of 1064 nm are amplified to an average output power of 42 W. Subsequently the pulses pass a non-linear crystal where part of the light is converted to green light (532 nm). The non-converted IR-power is partly used to synchronously pump an OPO and partly used for sum frequency mixing (SFM) with the OPO output at 1535 nm. The generated red light (628 nm) is either mixed with the non-converted signal radiation to generate blue light at a wavelength of 446 nm or transmitted to yield the red output.

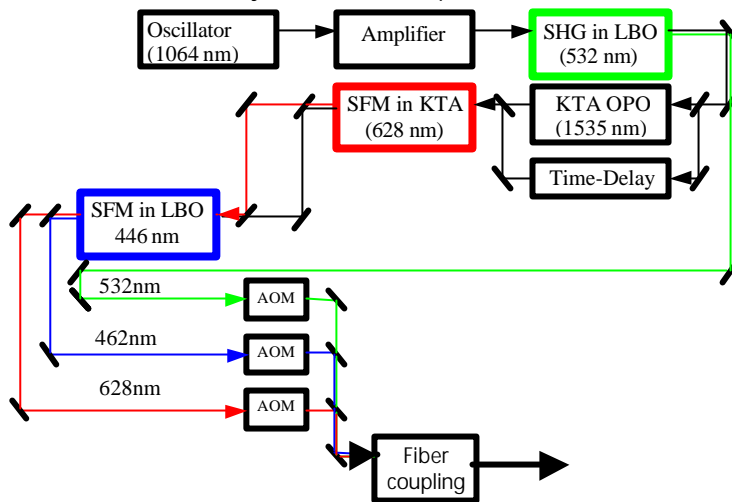


Fig. 3 Principal schematic of the laser head

A modelocked laser is used in the RGB system for two reasons: much higher peak intensities compared to continuous wave (cw) lasers are achieved, which are necessary for efficient non-linear frequency generation. Secondly, provided the pulses are short enough (≈ 10 ps), no speckles are visible on the screen because of a broad spectrum and hence, the short coherence length.

2. FIBER COUPLED DIODE LASER PUMPING MODULE

Fiber coupled diode lasers are used as the pumping source for the RGB laser. By beam shaping of a diode array and then coupling the radiation into an optical fiber a flexible pumping source can simply be adapted to the oscillator and amplifier active elements. Through collimation of the fast axis of the laser beam and rearrangement of the beam by a pair of step mirrors, we coupled the emission of one high power diode laser array into an optical fiber of 600 μm core diameter and 0.22 N.A. The selected fiber coupling concept adds some important advantages to the RGB laser system. The use of micro optics and quartz-quartz fibers guarantees long term stability of the laser parameters, a high coupling efficiency and allows for the separation of the fiber at the diode mount.

2.1. Beam rearrangement

The high power diode lasers for cw operation are implemented as 10 mm wide semiconductor bars that are mounted to a heat sink and emit up to 30 W of cw optical power. There are distinct emission regions, each 150 μm wide, distributed along the laser bars with a filling factor of 30 %. The divergence angle along this axis ('slow axis') is approximately 10° (90 % power content). The height of the emitters is approximately 1 μm , corresponding to high divergence angle (about 80° at 90 % power content) along that direction ('fast axis'). Calculating the beam parameter products (BPP) along the two axes one obtains 0.3 to 0.5 $\text{mm}\cdot\text{mrad}$ for the fast axis and approximately 500 $\text{mm}\cdot\text{mrad}$ for the slow axis. To generate a circularly shaped beam suitable e.g. for fiber coupling, the BPP has to be made symmetrical. For rearrangement of the laser beam we apply a concept based on a pair of step mirrors^{2,3,4}. This concept is licensed to JENOPTIK Laserdiode GmbH (JO LD) by the Fraunhofer Institute for Laser Technology in Aachen, Germany.

2.1.1. Fast axis collimation

In a first step the highly divergent radiation of the diode laser bar in the 'fast' direction is collimated by a cylindrical micro lens. Generally, there are no perfect lenses available that preserve the BPP. The utilization of high-refractive index aspheric lenses allow for the collimation of the fast axis to 5 mrad at a beam height of 0.6 mm with high efficiency equivalent to a BPP of 0.8 $\text{mm}\cdot\text{mrad}$. The slow axis is not affected by this collimation.

2.1.2. Rearranging of the laser radiation

A pair of identical step mirrors with 13 steps divides the collimated radiation into 13 subbeams along the slow axis and arranges them one below the other. The BPP along the slow axis is diminished by a factor of 13 to approximately 38 $\text{mm}\cdot\text{mrad}$ whereas along the fast axis it is increased by the same factor to 20 $\text{mm}\cdot\text{mrad}$. The rearranged beam is much more symmetric regarding the BPPs than the radiation emitted directly from the diode laser (Fig. 4).

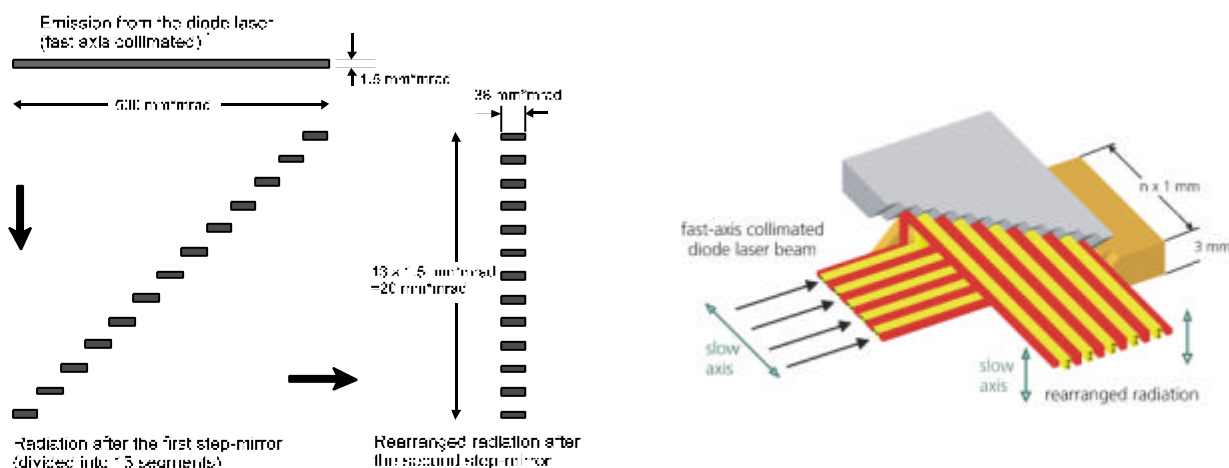


Fig. 4 Scheme of symmetrization of BPP of a diode laser bar by means of a pair of step-mirrors. The first step mirror divides the 10 mm wide emission into 13 parts and shifts these along a 45° line (lower left). The second step mirror shifts the 13 parts so they are positioned one above the other.

2.1.3. Slow axis collimation and fiber coupling

The slow axis is collimated by a conventional cylindrical lens ($f = 40 \text{ mm}$) after the reordering of the step-mirrors. The result is a collimated beam of rectangular shape that can be focused ($f = 20 \text{ mm}$) into an uncoated optical fiber. The fiber diameter and the numerical aperture are determined by the BPP of both symmetrical axes.

2.2. Diode parameters and operating characteristics

The pumping diode was developed as a pump source for the RGB laser head. The parameters (Table 2) are adapted to the special requirements of this application, but can be modified in terms of the wavelength, output power, monitoring, cooling system etc.

Center wavelength	808 nm \pm 1.5 nm
Spectral breadth	< 4 nm (90 % power content)
Fiber coupling	600 μm core, N.A. 0.22
Fiber output power	20 Watt
Threshold current	8 ... 10 A
Slope fibre output	> 0.8 W/A
Coupling efficiency	> 75 %
Monitoring inside of the housing	PIN – Photodiode

Table 2 Laser diode parameters.

The laser diodes and the beam shaping optics are mounted on a copper plate and the housing is hermetically sealed. Peltier thermo electric elements are integrated into the mount. By means of pulse width modulation the temperature is stabilized to 0.1 K.

The life time of the laser diode bars for cw-operation at an output power of 50 W has been investigated and determined to be > 20,000 hours (Fig. 5). In the RGB laser system the diodes are typically operated at an output power of the diode bar of 16 W. Several aspects can influence the degradation behavior. Early failures of laser diodes are regularly identified during the burn-in tests. The cooling and control system as well as the mounting technology for all components guarantees heat dissipation and constant temperature of the laser bar over the whole life time. A hermetically sealed housing prevents degradation due to humidity or chemical vapors. A life time test with the plug-in unit of the RGB laser system including 9 fiber coupled laser diodes (Fig. 6) is in progress.

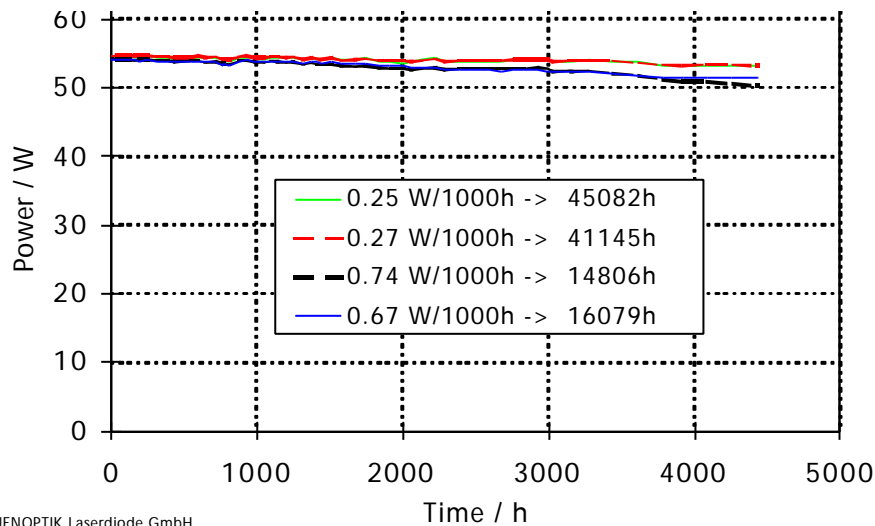


Fig. 5 Lifetime measurement of laser diodes at 808 nm

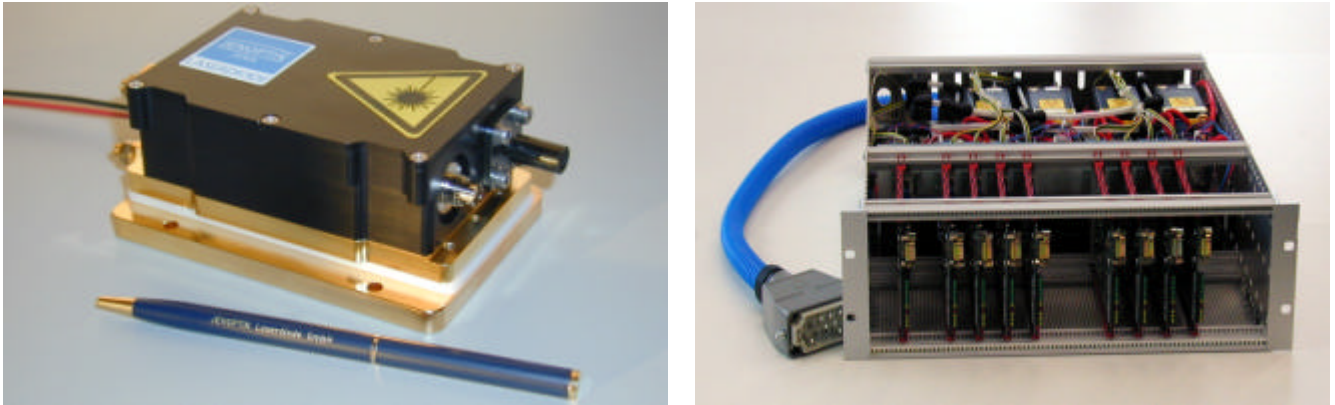


Fig. 6 Fiber coupled module with integrated TEC and the plug-in unit with 9 fiber coupled laser diodes

3. MODELOCKED OSCILLATOR

The modelocked oscillator is pumped by a fiber coupled diode laser. The fiber core size is 600 μm and the power content is 99.6 % at a numerical aperture of 0.22. The laser crystal is longitudinally pumped to match the pump beam to the laser beam. The mode size of the fiber is focused with a 1:1.1 optics to a beam diameter of approximately 660 μm inside the laser crystal which is slightly smaller than the calculated mode size in the laser crystal. The output beam is TEM_{00} with a measured M^2 -value of 1.0 in both directions (Fig. 7).

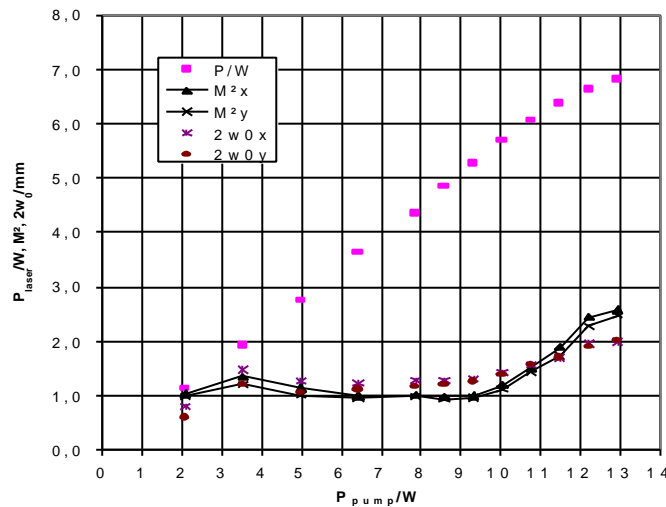


Fig. 7 Oscillator output power and beam quality

The active material is a 8 mm long Nd:YVO_4 crystal with a Nd atomic concentration of 0.7 %. Nd:YVO_4 was chosen because of the high gain emission cross section ($\sigma = 15.6 \cdot 10^{-19} \text{ cm}^2$ at 1.1 atomic %, a-cut), the broad absorption bandwidth (15.7 nm) which makes it an ideal candidate for diode pumping, and the broad emission bandwidth of 1.0 nm which supports pulse widths below 10 ps¹⁵. Pulse widths in the fs-regime would be attainable with Nd:glass materials, but this would dramatically increase the demands on the stability of the length adjustments of the synchronically pumped OPO and the subsequent non-linear processes. A disadvantage of Nd:YVO_4 is the high thermal lensing coefficient h with

$$h = \frac{\alpha}{k} \frac{dn}{dT}$$

where α is the absorption coefficient, κ the thermal conductivity, and dn/dT the change in refractive index as a function of the temperature. With $\alpha = 31.4 \text{ cm}^{-1}$ (at 808 nm and 1.1 % atomic %, a-cut), $\kappa = 5.1 \text{ W/(m}\cdot\text{K)}$, and $dn/dT = 3 \cdot 10^{-6} \text{ K}^{-1}$ (at 808 nm and 1.1 % atomic %, a-cut), a thermal lensing coefficient of $h = 1.8 \cdot 10^3 \text{ W}^{-1}$ is obtained which is theoretically four times bigger in comparison to Nd:YAG¹⁵. For this reason, special care was taken to design the resonator to be as stable as possible against thermal lensing effects, i.e., the resonator was optimized with respect to the invariance of the mode size in the laser crystal against changes in the strength of the thermal lens. For a thermal lens between 300 and 1,100 mm effective focus length, the mode size changes by only 10 %.

Passive modelocking with a semiconductor saturable absorber was chosen^{5,6} to guarantee the stability and robustness which is necessary for industrial applications. Using enhanced spatial hole-burning^{7,8} a minimum pulse width of 6 ps was achieved (Fig. 8). If the laser crystal was moved away from the mirror, the pulse widths increased up to a factor of 2. Depending on the design of the saturable absorber and the mode size on the sample the modelocked Q-switching threshold was measured to be between 0.5 W and 2 W⁹.

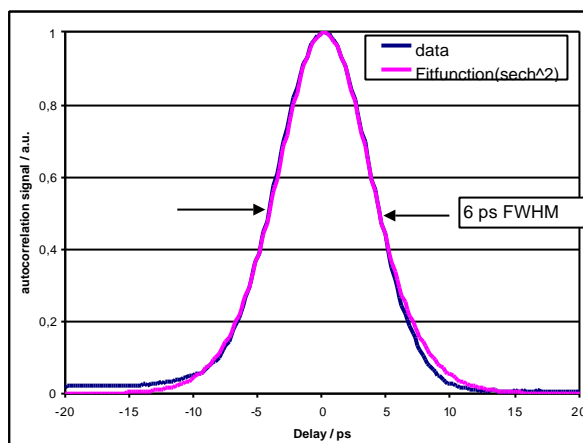


Fig. 8 Autocorrelation signal of oscillator pulse

The ratio between the modelocked IR-output power (4.5 W) and the pump power at the fiber end (10 W) was 45 %. The diode was operated at 22 A and 1.9 V, i.e. the total electrical to optical efficiency was 10.8 %. Due to the broad absorption bandwidth of Nd:YVO₄ the output power of the laser was stable up to +/- 0.5 % for a realized temperature stability of ± 0,2 K.

The geometrical size of the oscillator is 700 x 80 mm². The resonator is stabilized to < 50 μm to guarantee the length stability of the oscillator-OPO system even without an active length control.

4. AMPLIFIER

The laser crystal Nd:YVO₄ has been described in the literature^{10,11,12,13,14} as an effective laser and amplifier laser material for continuous wave, high repetition rate Q-switched and modelocked TEM₀₀ laser operation. Laser designs include longitudinal pumped rods, side pumped slabs and the thin disc laser approach.

The design of Nd:YVO₄ amplifiers must also consider the low thermal conductivity of Nd:YVO₄. Consequently an approach with 4 amplifier stages has been chosen in this work. The amplifiers are longitudinally pumped. Total optical efficiency of the amplifier stages is about 40 %.

The output power of the modelocked oscillator is 4.5 W. The Faraday isolator is used to isolate the oscillator from feedback to obtain stable modelocking. The first amplifier stage has an amplification of 2.5 leading to an output power of about 12 W. The second to fourth amplifier are operating in gain saturation, thus leading to additional 10 W of output power per stage, resulting in a total power of 42 W at the output beam of the amplifier system.

To achieve high efficiency and beam quality simultaneously, a careful matching between the output beam waist of the oscillator and the optimum beam waist of the amplifier stages has to be considered. Additionally the intensity of the input beam of the amplifiers has to be optimized for maximum gain.

The beam path in the amplifier system has been carefully modelled by using of FEM and commercial beam propagation software. Modematching is such that it leads to a waveguide structure of modematching lenses and the thermal lenses inside the laser crystals act as focusing elements. The focal length of the laser crystals is in the order of 120 mm. The beam waist of the output beam is $2\omega_0 = 0.5$ mm. The experimental beam parameters correspond to the calculated values to better than 10 %. The output beam parameters are $M^2 = 1.2$, measured with a *Coherent* Modemaster, the output power being 42 W. The complete amplifier system is integrated on a breadboard with a footprint of 330 x 240 mm².

5. OPTICAL PARAMETRIC OSCILLATOR (OPO)

The key component for generation of red and blue light is the synchronously pumped noncritically phase-matched potassium titanyl arsenate (KTA) optical parametric oscillator (OPO) as described in ¹⁶.

The signal resonant OPO cavity is generating a signal wave at 1535 nm and an idler wave at 3470 nm. Whereas the idler wave is not used for further frequency conversion the signal output is essential to the generation of red (629 nm) and blue (446 nm) light. Therefore stable operation of the OPO is an important demand. Since the OPO is synchronously pumped one has to avoid any length mismatch between the OPO and the laser resonator.

The influence of OPO resonator length changes on the signal pulse power and duration is shown in Fig. 9. In this figure, the point $\Delta L = 0$ (no length mismatch) is determined by the maximum of the signal power. The power and pulse duration are normalized to the values at this point. The behavior of the dependencies as depicted in Fig. 9 can be explained by the change of the overlap of the resonant signal pulse and the pump pulse in the KTA crystal and taking into account different group velocities of the interacting signal, idler and pump pulses within the crystal.

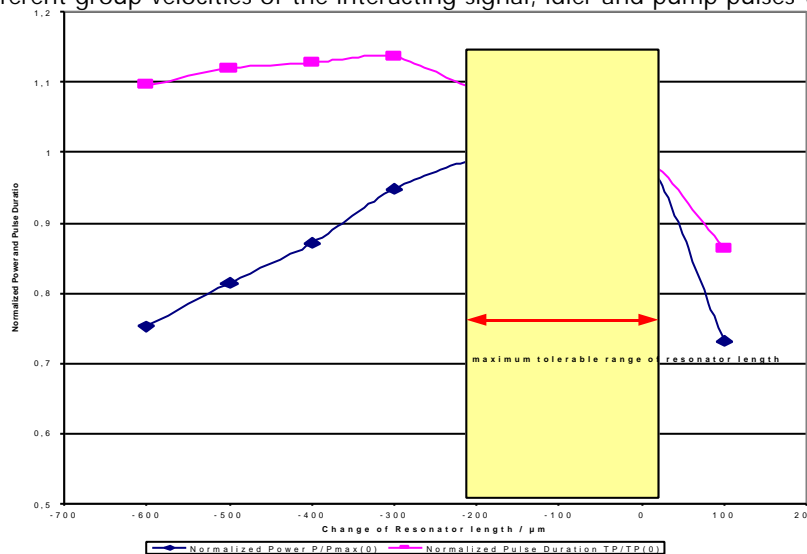


Fig. 9 Measured signal pulse duration and power in dependence of OPO resonator length changes

The allowed resonator length change ΔL_{acc} can be estimated by the condition that the power drop must be less than 5 % and the pulse duration increases less than 10 % which is important for the subsequent frequency mixing processes. From Fig. 9, it follows that the overall tolerable resonator length change is approximately 200 μm . Accordingly, the maximum allowed length variations of the folded resonator has to be smaller than 50 μm . To operate within the allowed length variation, a thermal stabilization of the aluminum base plate (thermal expansion coefficient about $25 \cdot 10^{-6}$) of ± 1 K is necessary.

Besides stable output the goal is an OPO efficiency $P(\text{signal})/P(\text{pump}) \geq 40\%$. This value corresponds to a pump pulse duration of about 7 ps (FWHM).

Use of the idler or non-converted pump wave is not possible. Due to the large wavelength difference, mode matching in the nonlinear crystal would be difficult to achieve and the temporal pulse shape of transmitted, depleted pump light is typically distorted and strongly depends on the OPO resonator length, i. e. further frequency mixing becomes unstable.

6. SUM-FREQUENCY GENERATION

The generation of the green beam is realized by single pass frequency doubling of 1.064 μm . The generation of 629 nm and 446 nm is achieved by sum frequency generation (SFM) as schematically depicted in **Fig. 10** and published in Ref.¹. Red radiation (629 nm) is generated by mixing the OPO signal (1.535 μm) with the laser radiation (1.064 μm) in a critically phase-matched KTA-crystal which has been proven to be the favorable nonlinear material (higher conversion efficiency than LBO, small walk-off angle of 0.1° which does not distort the beam profile). The blue beam (446 nm) is produced by SFM of the red light with the residual OPO signal radiation in a critically phase-matched LBO crystal which turned out to be the best material in comparison with BBO and RTA (no absorption, small walk-off angle of 0.6°).



Fig. 10 Nonlinear frequency conversion unit with dimensions of 370 x 340 mm².

It is reasonable to start with given RGB powers as fixed in the specs (7.0/6.5/4.8 W) and to look backwards what overall laser power is needed. This is illustrated in the 3-D-plot of **Fig. 11**. The surface depicts the laser power which is necessary to reach the RGB power specifications depending on the efficiency of sum frequency mixing processes "red" (η_{red}) and "blue" (η_{blue}) for a given OPO efficiency of 45%. For small η_{red} , η_{blue} a very high value of laser power is necessary, but the slope is decreasing quickly for increasing efficiencies and running out relatively flat for efficiencies > 50%. A pump power at the 40-W-level and below which is indicated as dark area in the surface plot of Fig. 11 is sufficient for ($\eta_{\text{blue}}, \eta_{\text{red}} \geq (30\%, 50\%)$). Both values are realized with our crystals at optimum focussing conditions. The overall efficiency of conversion from 1.064 μm to RGB is thus nearly 50%.

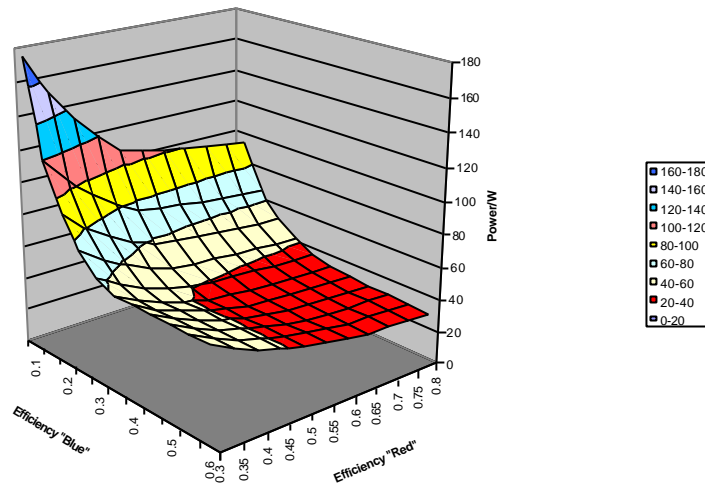


Fig. 11 IR laser power for specified RGB output in dependence of efficiencies of SFM processes for OPO efficiency of 45 %

7. MODULATION UNIT

The modulation of RGB light is realized by acusto-optical modulators (AOM) instead of previously used electro-optical modulators (EOM). A very high contrast ratio of better than 1:1,000 (EOM: < 1:500), a small modulation voltage of about

1 V (EOM: 200 V), small dimensions of about 10 cm³ only (EOM: 50 cm³) and easier alignment are the advantages of AOM over EOM. The AOM has a carrier frequency of 180 MHz and a diffraction efficiency of 75 %. The red, green and blue beams are modulated with a maximum frequency of 32 MHz. Fig. 12 shows the modulation unit which includes the AOMs, the white light balancing, an active angle and position stabilization system of the three beams and the fiber coupling optics.

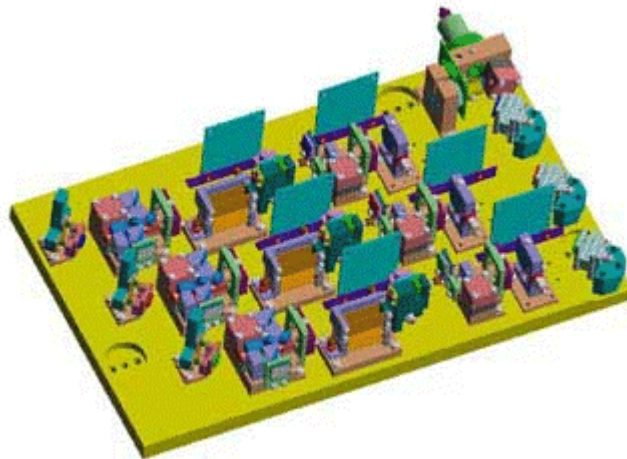


Fig. 12 Modulation unit with dimensions of 300 x 500 mm²

8. OPTO MECHANICAL DESIGN CRITERIA

Different materials have been tested with respect to angle stability as a function of temperature. The objective of these experiments was to find a highly mechanically and thermally stable mirror mount. Four different types of two-axis flexure mounts were tested. The first type (type I) was machined from a single piece of high-grade steel (X5CrNi18.10). Type II - IV were made from two pieces of metal, mounted together with 4 screws. Type II was made from aluminum (AlMg4,5), type III from brass (CuZn39Pb3), and type IV from high-grade steel (X5CrNi18.10).

To measure the thermal stability, the mounts were exposed for several times to a temperature shift from + 25 °C to – 25 °C or from + 25 °C to + 75 °C, kept at this temperature for one hour, and then heated (cooled) back to the original temperature of + 25 °C. Before and after each temperature cycle, the tilt between the mirror and a reference plane was measured with an autocollimating telescope. On average (heat and cooling exposures, x- and y-plane, different test cycles) the mean square deviation was 0.63 arc minutes for type I, 0.32 arc minutes for type IV, 0.054 arc minutes for type II and 0.022 for type III, i.e., the hysteresis effect after temperature cycles of brass and aluminum is about an order of magnitude better than with steel. Note that this is not a measure for the angle tilt in warm or cold environment, but a measure for how good the system returns its original state after exposure to cold or warm conditions (during transport or storage). The whole system is mounted on a base plate, which is temperature stabilized during operation.

To determine the relationship between the mechanical stability and the stability of the lasing system we measured the stability of the output power as a function of the angle misalignment for a folding mirror. A power degradation of 5 % occurred at a tilt angle of 1 arc minute. It can be concluded that hysteresis effects of the mirror mounts are well below the critical values of major changes in the laser output power.

To check the mechanical stability we performed a number of vibration- and shock tests (**Table 3**):

	Shock	Continuous shock	Vibration
Stimulation	half-sinusoidal	Half-sinusoidal	Sinusoidal with sliding frequency
Load	30 g/6 ms	10 g/6 ms	0.15 mm/2 g
Quantity	3 per direction	1000 per direction	10 cycles per direction
Direction	2 (+/- position of use)	2 (+/- position of use)	1 (position of use)
Rate			1 octave/min
Frequency			10 Hz – 2000 Hz – 10 Hz (1 cycle)

Table 3: Tests for mechanical stability.

All types showed comparably good results: type I – 0.13 to 0.32 arc minutes, type II – 0 to 0.067 arc minutes, type III – 0.067 to 0.13 arc minutes and type IV – 0.13 arc minutes. In general, the effects due to mechanical stress were by an order of magnitude smaller than thermal effects. Again, aluminum and brass showed slightly better results, compared to steel.

9. SUMMARY

An industrial all-solid state Red-Green-Blue laser system for large image projection systems is presented. The start of serial production is scheduled for the summer of 2000.

10. ACKNOWLEDGMENTS

This work was carried out by a contract with Laser-Display-Technologie GmbH and supported by the Ministry of Economy of the German State of Thuringia. The authors gratefully acknowledge fundamental work by R. Wallenstein and his colleagues and the helpful discussions with C. Deter and J. Kraenert.

REFERENCES

1. A. Nebel, B. Ruffing, R. Wallenstein, "A high power diode-pumped all-solid-state RGB laser source", in *Conference on Lasers and Electro-Optics*, Vol. 6, 1998 OSA Technical Papers Series (Optical Society of America, Washington D.C., 1998), Postdeadline Papers CPD3.
2. K. Du, M. Baumann, B. Ehlers, H.G. Treusch, P. Loosen: "Fiber-coupling technique with micro step-mirrors for high-power diode lasers bars", *OSA TOPS Vol. 10* (C.R. Pollack, W.R. Bosenberg, eds.), pp. 390-393, 1997.
3. M. Baumann, B. Ehlers, M. Quade, K. Du, H.G. Treusch, P. Loosen, R. Poprawe: "Compact fibre-coupled high-power diode-laser unit", *SPIE Vol. 3097* (L.H.J.F. Beckmann, ed.), pp. 712-716, 1997.
4. Patent no. DE 44 38 368 (1996) and international applications.
5. U. Keller, D. A. B. Miller, G. D. Boyd, T. H. Chiu, J. F. Ferguson, M. T. Asom, "Solid-state low-loss intracavity saturable absorber for Nd:YLF lasers: an antiresonant semiconductor Fabry-Perot saturable absorber," *Optics Lett.*, vol. 17, pp. 505-507, 1992.
6. L. R. Brovelli, I. D. Jung, D. Kopf, M. Kamp, M. Moser, F. X. Kärtner, U. Keller, "Self-starting soliton modelocked Ti:sapphire laser using a thin semiconductor saturable absorber," *Electronics Lett.*, vol. 31, pp. 287-289, 1995.
7. B. Braun, K. J. Weingarten, F. X. Kärtner, and U. Keller, "Continuous-wave modelocked solid-state lasers with enhanced spatial hole-burning, Part I: Experiments," *Applied Physics B*, vol. 61, pp. 429-437, 1995.
8. F. X. Kärtner, B. Braun, and U. Keller, "Continuous-wave modelocked solid-state lasers with enhanced spatial hole-burning, Part II: Theory," *Applied Physics B*, vol. 61, pp. 569-579, 1995.
9. F. X. Kärtner, L. R. Brovelli, D. Kopf, M. Kamp, I. Calasso, U. Keller, "Control of solid-state laser dynamics by semiconductor devices," *Optical Engineering*, vol. 34, pp. 2024-2036, 1995.
10. W.L. Nighan, Jr., N. Hodgson, "Quantum-limited 35 W, TEM₀₀, Nd:YVO₄ laser", in *Conference on Lasers and Electro-Optics*, OSA Technical Papers Series (Optical Society of America, Washington DC, 1999), p.1
11. L. Gonzales, K. Kleine, L. Marshall, "High Brightness MOPA", in *Conference on Lasers and Electro-Optics*, OSA Technical Papers Series (Optical Society of America, Washington DC, 1999), pp.1-2.
12. G. Hollemann, H. Zimer, A. Hirt, "Pulsed-mode operation of a diode-pumped Nd:YVO₄ thin disc laser", in *Conference on Lasers and Electro-Optics*, Vol. 6, 1998 OSA Technical Papers Series (Optical Society of America, Washington D.C., 1998), pp. 543-544.
13. K.J. Snell, D. Lee, J.G. Manni, "High-Average Power, High-Repetition Rate, Side-Pumped Nd:YVO₄ Slab Laser MOPA System", in *Conference on Lasers and Electro-Optics*, OSA Technical Papers Series (Optical Society of America, Washington DC, 1999), Postdeadline Papers CPD1.
14. J.E. Bernard, A.J. Alcock, "High-repetition-rate diode-pumped Nd:YVO₄ slab laser", *Optics Letters* **19**, 1861 (1994).
15. W. Koechner, "Solid State Laser Engineering", Springer Series in Optical Sciences, A.L. Schawlow, A.E. Siegman, T. Tamir, eds., Fifth Edition, Springer Berlin, 1999, pp. 48-61.
16. B. Ruffing, A. Nebel, R. Wallenstein, Paper MF3-1, "High-Power all-solid-state cw mode-locked picosecond KTA optical parametric oscillator", Advanced Solid-State Lasers, 12th Topical Meeting, Jan. 27-29, 1997, Orlando, Florida.